Site-directed mutagenesis, *in vivo* electroporation and mass spectrometry in search for determinants of the subcellular targeting of Rab7b paralogue in the model eukaryote *Paramecium octaurelia*

E. Wyroba, P. Kwaśniak, K. Miller, K. Kobyłecki, M. Osińska

Nencki Institute of Experimental Biology of Polish Academy of Sciences, Warsaw, Poland

Abstract

Protein products of paralogous genes resulting from whole genome duplication may acquire new functions. The role of post-translational modifications (PTM) in proper targeting of *Paramecium* Rab7b paralogue (distinct from that of Rab7a directly involved in phagocytosis) was studied using point mutagenesis, proteomic analysis and double immunofluorescence after *in vivo* electroporation of the mutagenized protein. Here we show that substitution of Thr200 by Ala diminished the incorporation of [P^{32}] by 37% and of [C^{14}]UDP-glucose by 24% into recombinant Rab7b_200 in comparison to the non-mutagenized control. Double confocal imaging revealed that Rab7b_200 was mistargeted upon electroporation into living cells in contrast to non-mutagenized recombinant Rab7b correctly incorporated in the cytostome area. Using nano LC-MS/MS to compare the peptide map of Rab7b with that after deglycosylation with a mixture of five enzymes of different specificity we identified a peptide ion at m/z=677.6^{3+} representing a glycan group attached to Thr200. Based on its mass and quantitative assays with [P^{32}] and [C^{14}]UDP-glucose, the suggested composition of the adduct attached to Thr200 is (Hex)1(HexNAc)1(Phos)3 or (HexNAc)1 (Deoxyhexose)1 (Phos)1 (HexA)1. These data indicate that PTM of Thr200 located in the hypervariable C-region of *Paramecium octaurelia* Rab7b is crucial for the proper localization/function of this protein. Moreover, the two Rab7 paralogues differ also in another PTM: substantially more phosphorylated amino acid residues are in Rab7b than in Rab7a.

Introduction

Divergence of genes arose by whole genome duplications (WGD) may endow their products with new functions.[1] Since it is known that post-translational modifications (PTMs) may affect protein interactions,[2] we tested whether PTMs could contribute to the neofunctionalization of the *rab7b* gene product in the model eukaryote *Paramecium octaurelia.* Based on extensive phylogenetic analyses comprising 210 proteins we reported earlier that Rab7 proteins evolved before the radiation of main supergroups of Eukaryota and are widely distributed in almost all of them.[3] We cloned two Rab7 genes from *Paramecium octaurelia*,[4] known to undergo at least three successive WGDs.[1,5]

Paramecium octaurelia Rab7a and Rab7b, displaying 62.3-63.3% identity with human Rab7,[6] have distinct localizations, expression and functions.[4] Silencing of Rab7a (M_r = 22.5 kDa) suppressed phagosome formation by 70% and impaired their acidification. Ultrastructural analysis with double immunogold labeling revealed that this effect was due to a lack of V-ATPase recruitment. During phagocytosis expression of Rab7a was almost 5-fold higher than that of Rab7b. Rab7b (M_r =25 kD) associated with microtubule bundles and structures supporting the oral apparatus.[4] No phenotypic effects of Rab7b depletion by RNAi have been noticed. In 2D gel electrophoresis two Rab7b immunoreactive spots of slightly different pI (~6.34 and ~6.18) were observed and a single spot of pI ~6.34 for Rab7a. Both ProQ Emerald staining and ConA overlay assay of immunoprecipitated Rab7b indicated its likely glycosylation in accordance with its faster electrophoretic mobility upon deglycosylation.[4]

The two *Paramecium octaurelia* Rab7 paralogues differ from each other by five amino acids out of 206: four in the C-terminal hypervariable region that participates in determination of specificity of Rab7 interactions with membranes, its localization within the cell[7] and is an important determinant of effector binding.[8] The fifth diverged amino acid residue in position 140 (Ser in Rab7b and Ala in Rab7a)[4,6] is located in the region of α-helix with the highest frequency of secondary structure elements.[3,9]

Based on *in silico* modeling (NetOGlyc 4.0 analysis tool)[10] Thr200 is the unique site in Rab7b that may undergo *O*-glycosylation distinguishing this protein from Rab7a. Therefore this amino acid was changed to alanine to prevent PTM and site directed mutagenesis was confirmed by LC-MS/MS. We looked into the details of this machinery in recombinant system and created the mutagenized form of Rab7b not undergoing PTM to follow its intracellular targeting and properties.

Correspondence: Prof. Elżbieta Wyroba, Nencki Institute of Experimental Biology of Polish Academy of Sciences, 3 Pasteur Street, 02-093 Warsaw, Poland.
Tel. +48.22.5892357 - Fax: +48.22.22532.
E-mail: e.wyroba@nencki.gov.pl

Key words: Point mutagenesis; electroporation; post-translational modifications; mass spectrometry; glycosylation; Rab7; *Paramecium*; recombinant proteins.

Contributions: EW, experiments concept and design, paper writing; MO, PK, KK, KM, EW, experiments performing; EW, PK, KM, MO, data analysis.

Conflict of interest: the authors report no conflics of interest.

Acknowledgments: We are grateful to Dr. Sci. Piotr Suder (Biochemistry and Neurobiology Department, AGH University of Science and Technology, Cracow, Poland) for valuable discussion on mass spectrometry.

Funding: this work was supported by statutory funds to the Nencki Institute of Experimental Biology of Polish Academy of Sciences and by grant N. N303 615038 from the Ministry of Science and Higher Education/National Science Centre.

Received for publication: 21 December 2015.
Accepted for publication: 21 March 2016.

European Journal of Histochemistry 2016; 60:2612
doi:10.4081/ejh.2016.2612

Materials and Methods

Reagents

All reagents were of the highest purity available from Sigma-Aldrich (St. Louis, MO, USA) unless otherwise stated.

Plasmid construction and site-directed mutagenesis

Since cDNA from *Paramecium octaurelia* cannot be used to express a protein in *E. coli* due to the different genetic code of Ciliates, a Rab7b coding sequence optimized for protein expression in *E.coli* flanked by EcoRI and XhoI sites was synthesized commercially (Mr. Gene GmbH, Regensburg, Germany). This sequence was introduced as EcoRI-XhoI fragment into the pET28b vector (Novagen, Merck KGaA,

Darmstadt, Germany) to create expression plasmid pRab7bHis. The amino acid sequence of the recombinant Rab7b was identical to that of the native protein cloned by us.[6] Substitution T200A was introduced in PCR reactions using primers: 5'-CCAAACAGGGTG-GTTGTTG and CCTGTTTTTTAGGATCCT-GTTTG. Phusion DNA polymerase was used in the reactions amplifying whole recombinant plasmid. The reaction mixtures were treated with DpnI endonuclease to remove template DNA and then the 5' ends of the PCR products were phosphorylated with T4 polynucleotide kinase and circularized with T4 DNA ligase. The recombinant plasmids were verified by sequencing.

Expression and purification of recombinant Rab7b proteins

The recombinant plasmids were introduced into *E.coli* BL21 (DE3) strain by transformation. Recombinant proteins were produced in mid-logarithmic cultures (OD_{600} >0.6) in LB medium with kanamycin (50 µg/mL) by induction for 5 h with 1 mM isopropyl β-D-1-thio-galactopyranoside (IPTG). Cultures were centrifuged, washed with STE buffer (150 mM NaCl, 1 mM EDTA, 10 mM Tris-Cl pH 8.0), resuspended in STE with 1 mM PMSF, spun and resuspended in buffer A (50 mM HEPES pH 8.0, 300 mM NaCl, 10% glycerol, 10 mM β-mercaptoetanol, 1 mM imidazole, 0.1% Triton X-100, 1 mM PMSF). After lysis in French press (20,000 psi) the lysate was spun at 39,000 x g for 1 h at 4°C and the supernatant was mixed with His-Select®Nickel Affinity Gel, incubated on ice for 1 h and spun (5000 x g, 5 min, 4°C).The resin was washed with 5 mL of buffer A, spun as above, loaded on Poly-Prep Chromatography Columns (Bio-Rad, Hercules, CA, USA) and washed, consecutively, with 5 volumes of each: buffer B (buffer A with 10 mM imidazole), buffer C (buffer B without Triton X-100), buffer D (50 mM HEPES pH 8.0, 2 M NaCl, 10 mM β-mercaptoethanol), buffer E (50 mM HEPES pH 8.0, 150 mM NaCl, 10 mM β-mercaptoethanol, 10% glycerol), buffer B and buffer F (buffer C with 20 mM imidazole). The $(His)_6$-tagged proteins were eluted with buffer G (buffer C with 250 mM imidazole) and their aliquots were run in 15% SDS-PAGE to assess purity.

Cell homogenate

Axenic culture (5-day-old) of *Paramecium octaurelia* (stock 299s) was spun down at 600 x g for 45 s, washed twice with MSS buffer (0.08 mM KH_2PO_4, 0.08 mM K_2HPO_4, 0.2 mM NaCl, 0.8 mM $CaCl_2$, 0.4 mM $MgCl_2$, pH 7.0, as described by Soldo *et al.*[11]) and left in MSS for 30 min at 16°C. After spinning down the cell homogenate was obtained as previously described.[4]

Electroporation

P. octaurelia culture prepared as above was resuspended in a fresh volume (100 mL) of MSS buffer for 60 min to prevent autofluorescence.[12] After spinning down and another wash cell viability was examined under a binocular microscope. The buffer G in which recombinant proteins were eluted from the affinity gel was exchanged as follows: 0.5 mL of Sephadex G-25 was loaded on the Spin-X centrifuge tube filters (0.45 µm, Costar Corning) and rinsed fivefold with 0.3 mL of MSS buffer followed by 1 min spin (1000 x g). Recombinant protein solution (130 µL) was overlaid on the column and spun for 4 min. Purified recombinant protein in MSS (50 µg in 50 µL) was mixed with 250 µL of *Paramecium* suspension (64,000 cells) in a 0.4 mm gap cuvette and electroporation was performed in a Gene Pulser II Electroporator (Bio-Rad) at the settings: 60 V, 200 µF, 300 Ω. After electroporation cells were transferred into sterile Eppendorf tubes and gently mixed for 4 h at 27°C (*i.e.*, under the cell cultivation conditions) and next processed for confocal imaging.

Confocal microscopy

Electroporated cells were fixed with 3.5% (w/v) freshly prepared formaldehyde (20 min) with gentle mixing, washed twice in PBS and blocked in 4% milk in PBS/0.1% Triton X-100 for 1 h. Labeling with primary antibodies (Ab): mouse monoclonal (1:200) against His_6-Tag (Applied Biological Materials Inc., Richmond, Canada) and rabbit monoclonal (1:45) against β-tubulin (Epitomics, Burlingame, CA, USA) for 2.5 h was followed by washing with PBS/0.1.% Triton X-100. Anti-mouse Ab conjugated with rhodamine at 1:100 (Polysciences, Inc., Warrington, PA, USA) and anti rabbit-FITC conjugated Ab at 1:50 (Molecular Probes) were used as secondary antibodies for 1 h. Samples were washed 6x with PBS, mounted in 2.5% 1,4-Diazabicyclo [2.2.2] octane in Mounting Medium and analyzed in a Leica TCS STED SP5 Spectral Confocal system (Leica Mikrosysteme, Vienna, Austria). Series of the single 0.2 µm optical sections were collected. The images were scanned at high resolution (with a 63x oil objective, 1.32 NA). Controls without the primary Ab produced no fluorescent signal.

Incorporation of [^{14}C]UDP-glucose

The experimental mixture was composed of a given recombinant protein in 50 mM Tris-HCl buffer, pH 7.4 and freshly prepared cell homogenate at 1:5 ratio (as measured by Bradford assay), 10 µCi of [^{14}C]UDP-glucose (ammonium salt, 250 mCi/mmol, Perkin Elmer, Norwalk, CT, USA) and 1 mM EGTA. The samples were incubated on a rotary mixer at 23°C for 45 min. Next, aliquot of His-Select® Nickel Affinity Gel was added at a 1: 2.5 (v:v) resin to the sample ratio and incubation was continued for 30 min at 4°C. The reaction mixture was transferred to a Corning® Costar® Spin-X® Plastic Centrifuge Tube Filter, centrifuged (6000 x g, 5 min, 4°C), washed twice with buffer A (60 µL/100 µL of sample) and spun as before. Elution buffer G was added (40 µL/100 µL of sample) and after 15 min of incubation the samples were centrifuged as before. Eluted recombinant protein (30 µL) was mixed with 1 mL of ULTIMA Gold cocktail (Perkin Elmer) for liquid scintillation counting in Beckman LS 6500 and 10 µL was taken for SDS PAGE. Mean values of radioactivity incorporation were calculated for duplicate samples. Protein bands stained with Ponceau S were quantified by GeneTools software (Syngene, Cambridge, UK).

In vitro glycosylation of Rab7b variants

Control experiments were performed before quantification of [^{14}C]UDP-glucose incorporation. Recombinant proteins and cell homogenate at 1:5 ratio were incubated in 50 mM Tris-HCl pH 7.4, 20 mM UDP-glucose (Abcam, Cambridge, UK) and 1 mM EGTA for 30 min at 23°C. Next purification of proteins was performed as above followed by SDS-PAGE, Con A overlay assay as previously described,[4] and Western blotting.

Incorporation of γ-[^{32}P] ATP by recombinant proteins

The reaction mixture comprised 50 mM Tris-HCl, pH 7.4 and 10 µCi γ-[^{32}P] ATP (Perkin Elmer), cell homogente and recombinant protein and incubation was performed for 30 min at 23°C. Aliquots of 10 µL of reaction mixtures were spotted onto P81 (Whatman) filters that were then washed 3x with 0.75% ortho-phosphoric acid followed by 95% ethanol,[13] air dried and quantified in a scintillation counter (Beckman LS 6500). After adding 5 mL of the ULTIMA Gold scintillator to each filter the second counting was performed immediately. Mean values of radioactivity incorporation were calculated from 3 series of experiments.

In the quantitative studies on [P^{32}] and [C^{14}] incorporation described above the ratio of the volume of His-Select® Nickel Affinity Gel to that of the reaction mixture was strictly controlled in each series of experiments. The efficiency of protein purification was followed by SDS-PAGE/Western blotting with anti-His and specific anti-peptide Rab7b antibody.

Western blotting

SDS electrophoresis and blotting was performed as previously described.[14] After Ponceau S staining detection of phosphorylat-

ed proteins was performed in 2 x PBS, 0.5% BSA, 1% PVP-10 (polyvinylpyrrolidone), PhosSTOP (Roche Diagnostic, Mannheim, Germany), 1% PEG 3500, 0.2% Tween 20) using anti p-Tyr (rabbit, P11230; BD Biosciences, St. José, CA, USA; 1:1000) or anti p-Ser (mouse, ALX-804-166-C100; Enzo Life Sciences, Farmingdale, NY, USA; 1:1000) followed by the respective secondary Ab: anti rabbit (1:4000) or anti mouse (1:1000). The protein bands were visualized by an ECL (Amersham Biosciences Hyperfilm ECL, GE Healthcare, Little Chalfont, UK). The film was scanned digitally with a Perfection 2450 Photo Scanner (Epson) and densitometry was performed using GeneTools software (Syngene). Images were processed using Adobe Photoshop CS4 and Illustrator CS4 (Adobe). Omitting of the primary Abs produced no bands.

Stripping was performed after each detection described above with Restore Plus Western Blot Stripping Buffer (Thermo Scientific) for 15 min and followed by washing with PBS containing 0.05 % Tween (PBST). Next immunoblotting was done with a specific antipeptide Ab[4] for Rab7b (1:600) in 4% milk in PBST followed by anti-rabbit Ab (1:4000). After subsequent stripping His-tagged proteins were revealed by incubation with monoclonal anti-polyHistidine Peroxidase Conjugate Clone HIS-1 (1:4000) in PBST with 1% bovine serum albumin for 1 h followed by triple wash with PBST and incubation with anti-mouse Ab as above.

Proteomic analysis

In-gel digestions was performed as previously described,[15] using one of the following enzymes in 50 mM NH_4HCO_3 buffer of varying pH: Trypsin-Gold, mass spectrometry grade (Promega, Madison, WI, USA) at pH=7.8 (500 fmol/μL), endoproteinase Asp-N from *P. fragi* at pH=7.0 (1 pmol/μL) and endoproteinase Lys-C, sequencing grade (Promega) at pH=8.0 (1.2 pmol/μL) at 37°C for at least 16 h. In a separate set of experiments endoproteinase Asp-N digestion was done and followed by nanoscale reverse-phase liquid chromatography/tandem mass spectrometry (nano LC-MS/MS). Then remaining peptides were additionally digested with trypsin. A search for glycosylated peptides was performed according to Noga *et al*.[16] on a Proxeon nanoLC chromatograph (Thermo Fisher Scientific, Vienna, Austria) connected on-line to an AmaZon ETD mass spectrometer equipped with a nanoFlow ESI ion source (Bruker, Bremen, Germany) using Bruker's HyStar, ver. 3.2 and TrapControl, ver. 7.1 software. For each LC separation in-house made columns were applied: precolumn ID 100 μm/length 1 cm, column ID 75 μm/length 10 cm, stationary phase: ReproSil C18 (Dr. Maisch GmbH, Ammerbuch-Entringen, Germany). Gradient used for nanoLC separation: 0 min/100% A; 40 min/45% A; 41 min/20% A; 42 min/20% A; 43 min/100% A; 45 min/100% A; solvents and flow rate as by Suder *et al.*[15] and mass spectrometer parameters as described by Drabik *et al.*[17]

Protein identification was performed using Mascot engine working as a part of the Proteinscape 2.1 software (Bruker, Bremen, Germany) with settings: taxonomy: all, enzymes: the type used for the cleavage, max 1 missing cleavage allowed, fixed modifications: carbamidomethylation, variable modifications: serine, threonine and tyrosine phosphorylation, methionine oxidation. SwissProt and Trembl databases were used for the initial identification. Then, for phosphorylation localization a database containing only *Paramecium octaurelia* Rab7a/Rab7b proteins was used. Glycosylation identification was based on the mass difference between glycosylated and deglycosylated peptides: the former are *invisible* for the Mascot system when the MW of the modification is unknown.

To confirm the site of glycosylation, proteins were deglycosylated with protein deglycosylation mix (V4931, Promega) according to the manufacturer's procedure. The peptide identification and assignment of post-translational modifications was performed by searching the data using the following constraints: only tryptic peptides with up to two missed cleavage sites were allowed; the results were filtered for peptide assignments; ±2.5 Da mass tolerance for peptide precursor mass searching; ±0.5 Da mass tolerance for the fragment ions. The whole procedure was carried out at the Biochemistry and Neurobiology Department of Materials Sciences and Ceramics Faculty, AGH University of Science and Technology, Cracow, Poland.

Results

Qualitative and quantitative studies on UDP-Glucose incorporation

Mutagenesis of Thr200 (the putative site of glycosylation in Rab7b) to alanine was confirmed by LC-MS/MS. To check whether glycosylation of the recombinant proteins occurs under our experimental conditions the recombinant proteins were incubated with cell homogenate and UDP-glucose followed by SDS PAGE and Con A overlay assay (Figure 1A). Subsequent Western blot analysis with anti-His Ab that was followed by stripping and reaction with anti-Rab7b specific Ab proved that $(His)_6$ Rab7b variants undergo glycosylation (Figure 1A). *In vitro* assay with [^{14}C]UDP-glucose indicated that its incorporation into $(His)_6$-Rab7b_200 was diminished by 24% relative to the incorporation into control $(His)_6$Rab7b (Figure 1B). Addition of 200 μM UDP-glucose to the reaction mixture diminished the incorporation of [^{14}C]UDP-glucose by 34%.

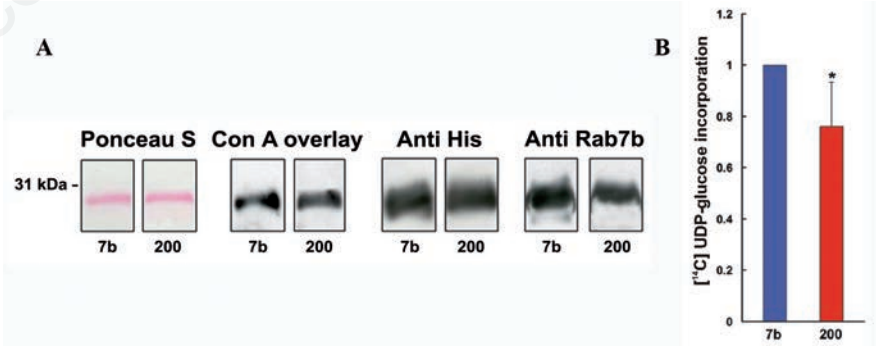

Figure 1. Recombinant Rab7b variants undergo glycosylation in the presence of *Paramecium octaurelia* cell homogenate and UDP-glucose or [C^{14}]UDP-glucose. A) Recombinant $(His)_6$Rab7b proteins were exposed to UDP-glucose and cell homogenate as described in Materials and Methods; after electrophoretic separation of the eluted proteins and Ponceau S staining, Con A overlay assay was performed followed by stripping and subsequent Western blotting with anti-His antibody and - after next stripping – with specific anti-Rab7b antipeptide antibody; molecular mass marker (kDa) is shown at the left. B) *In vitro* assay with [^{14}C]UDP-glucose, recombinant variants and *Paramecium* homogenate; incorporation into $(His)_6$Rab7b_200 as compared with the control $(His)_6$Rab7b; densitometry of bands; intensities of the $(His)_6$Rab7b_200 protein bands of the Coomassie Blue stained SDS PAGE were calculated as relative optical density *vs.* $(His)_6$Rab7b as the control sample. Asterisk indicates significant difference from $(His)_6$Rab7b at P<0.1, n=4.

Glycosylation analysis by nanoLC-MS/MS

Glycosylation of Thr200 was revealed by nanoLC-MS/MS analyses of the peptides maps derived by digestion of recombinant Rab7b constructs with endoproteinase Asp-N that was followed by cleavage with trypsin as described in Materials and Methods. After careful comparison differences like those exemplary shown in Figure 2 were evident: an additional peptide ion at m/z=677.6^{3+} was clearly detected in the (His)$_6$Rab7b recombinant protein that was glycosylated with UDP-glucose (Figure 2A, arrow) which was absent in the control (His)$_6$Rab7b sample incubated without UDP-glucose in the same experiment (Figure 2B).

To confirm this result, glycosylated (His)$_6$Rab7b samples were deglycosylated as described in Materials and Methods and again subjected to MS analysis. The peptide ion at m/z=677.6^{3+} was no longer detectable. The fragmentation spectrum of the 677.6^{3+} ion (Figure 2) was verified manually to check for the presence of fragment ions corresponding to the amino acid sequence of the Rab7b protein. As shown in Figure 3, the MS/MS spectrum reveals b- and y-ion series of the [195-206] peptide and an additional set of fragment ions representing hybrids of the peptide and a glycan group. The molecular mass of the glycan group was calculated at 624.2 Da based on the difference between the mass of the detected peptide (2029.8 Da) and the calculated mass of non-glycosylated [195-206] peptide with carbamidomethylated cysteine residues equal to 1405.6 Da.

GlycoMod software (http://web.expasy.org/glycomod)[18,19] was used for estimation of the nature of the glycan groups attached to the analyzed peptides. As concerns the adduct of 624.1 Da attached to Thr200 the most likely glycan modifications are the following:

i) (Hex)1 (HexNAc)1 (Sulph)3;
ii) (Hex)1 (HexNAc)1 (Phos)3;
iii) (HexNAc)1 (Deoxyhexose)1 (Sulph)1 (HexA)1;
iv) (HexNAc)1 (Deoxyhexose)1 (Phos)1 (HexA)1.

The following phosphoglycosylations are the most likely: (Hex)1(HexNAc)1(Phos)3 or (HexNAc)1 (Deoxyhexose)1 (Phos)1 (HexA)1, with a high preference for the presence of three phosphate groups as in the former case. This conclusion is based on the results indicating a significant decrease in the incorporation of both the [^{14}C]UDP-glucose (Figure 1B) and [^{32}P] into Rab7b_200 (Figure 4B) as compared with the control Rab7b. Three other detected glycosylations of Rab7b at Ser101, Thr131 (and most probably at Ser138) that do not differentiate Rab7a from Rab7b were also found using the same approach.

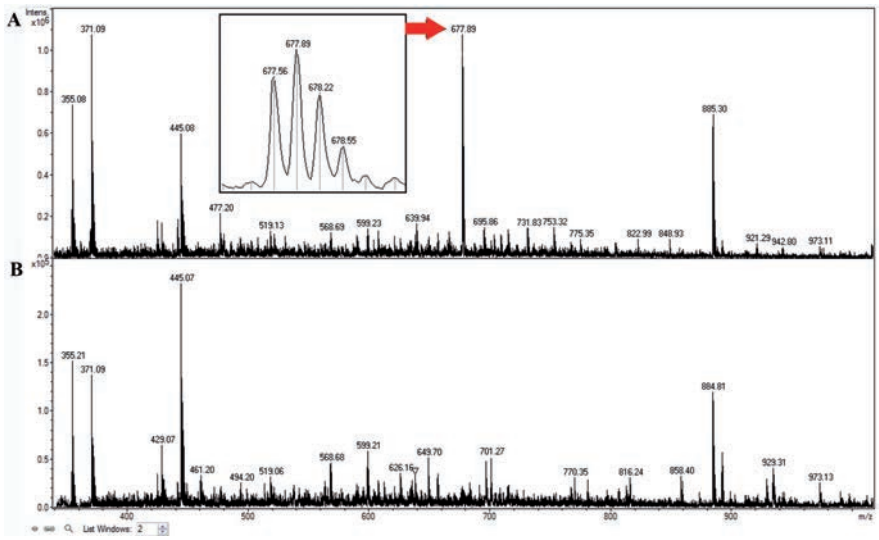

Figure 2. Comparison between averaged spectra from the nanoLC-MS separation of glycosylated (His)6Rab7b after UDP-glucose incorporation as described in Materials and Methods (A) with the control recombinant (His)6 Rab7b incubated without UDP-glucose under the same experimental conditions (B). There is the peptide ion at a mass to charge (m/z) ratio of = 677.6 in the spectrum (A, red arrow) not detected after deglycosylation (B). Inset in (A) shows a blow-up of this peptide ion. Isotopic pattern allows for estimation of ionization ratio as 3+. Both averaged spectra obtained by the accumulation of ca. 40 scans acquired within retention time: 21.4-22.2 min.

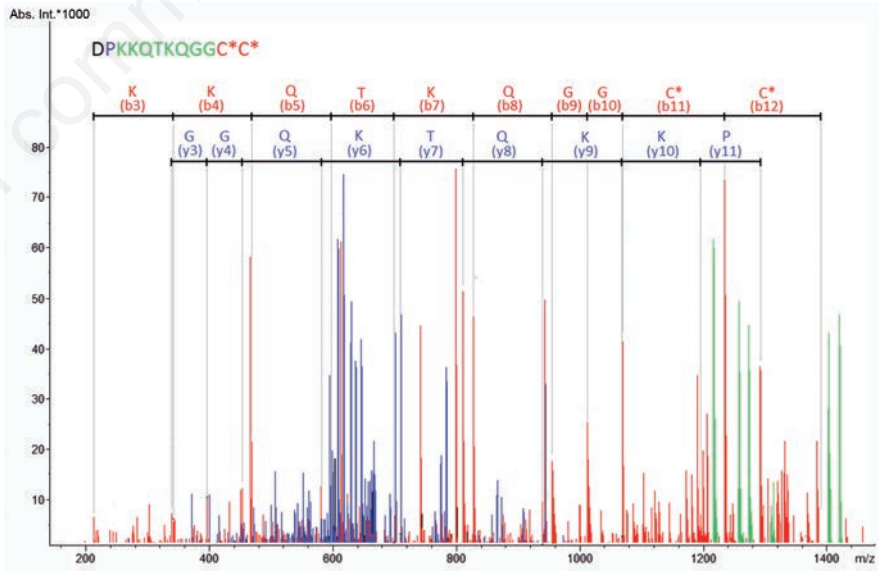

Figure 3. MS/MS spectrum derived after fragmentation of the 677.63^{+} ion detected in glycosylated Rab7b shown in Figure 2. Blue ions: come directly from the spectrum, red ions are derived after deconvolution of the blue ions; green ions: most likely represent hybrids of glycan modification and peptide fragments. In the upper part of the spectrum b-ions and y-ions are marked with corresponding amino acid residues. Additionally, identified sequence of the [195-206] peptide is shown: identification of the exact amino acid residues was based on y-ions (blue residue), b-ions (red residues) or both series (green residues). Black font indicates the single unidentified residue.

In vitro phosphorylation

We have previously reported the presence of 8 phosphorylated amino acids in endogenous Rab7a and Rab7b proteins,[4] and proved now that recombinant Rab7b constructs undergo *in vitro* phosphorylation using antibodies against phosphorylated amino acids (Figure 5).

As shown in Figure 4B incorporation of [P^{32}] was significantly decreased by 37% in the case of $(His)_6$ Rab7b_200 in comparison to that of the control $(His)_6$ Rab7b.

Analysis of phosphorylation by nano LC-MS/MS

Taking the advantage of the recombinant Rab7 variants undergoing *in vitro* phosphorylation as shown in Figures 4 and 5, additional proteomic analyzes were carried out in an attempt to identify all the amino acid residues undergoing this PTM. Figure 6 shows comparison of the phosphorylation patterns of Rab7a and Rab7b.

There are altogether 18 phosphorylated residues in Rab7b and 16 of them are also phosphorylated in Rab7a. Most of them are located in the Rab-specific motifs [9,49]: 14 in Rab7b (including five serine residues) and 13 in Rab7a. Interestingly, there is no such PTM in Rab7a in the RabSF3, while in Rab7b both Ser98 and Ser101 are phosphorylated (Figure 6). Similarly, in the RabSF4 motif three residues are phosphorylated in Rab7b (Ser176, Thr187 and Thr188) and only one in Rab7a (Thr187). As concerns the conserved motifs involved in binding/coordination of Mg^{2+} with phosphate groups, Thr22 in PM1 is phosphorylated in the both proteins, while Ser17 only in Rab7a.

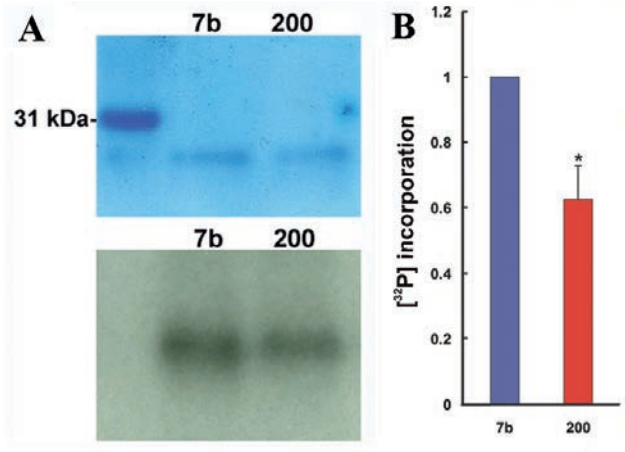

Figure 4. Incorporation of [^{32}P] into recombinant $(His)_6$Rab7b and its mutagenized form $(His)_6$Rab7b_200 in the presence of *Paramecium octaurelia* cell homogenate. A) Upper panel, Coomassie stained gel (MW marker at the left); lower panel, autoradiogram. B) Equal volumes of eluted recombinant proteins were immediately analyzed in a scintillation counter and their identical aliquots subjected to SDS PAGE; densitometry of bands; intensities of the $(His)_6$Rab7b_200 protein bands were calculated as relative optical density *vs* $(His)_6$Rab7b control samples. Asterisk represents a significant difference from the control sample at P<0.01 by Student's *t*-test, n=3.

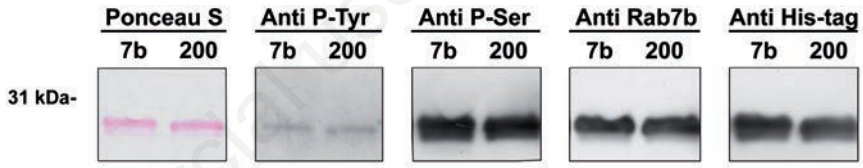

Figure 5. Recombinant (His_6) Rab7b variants undergo *in vitro* phosphorylation. The same blot analysis using antibodies against phosphorylated amino acids. The experiment was conducted as described in Figure 1A. After electrophoretic separation of eluted affinity purified proteins by 15% SDS PAGE and Ponceau Red staining, Western blotting was performed sequentially with anti P-Tyr, anti P-Ser, anti His-tag and anti-Rab7b specific antipeptide Ab. Stripping at each step was performed as described in Materials and Methods. Molecular mass marker is shown at the left.

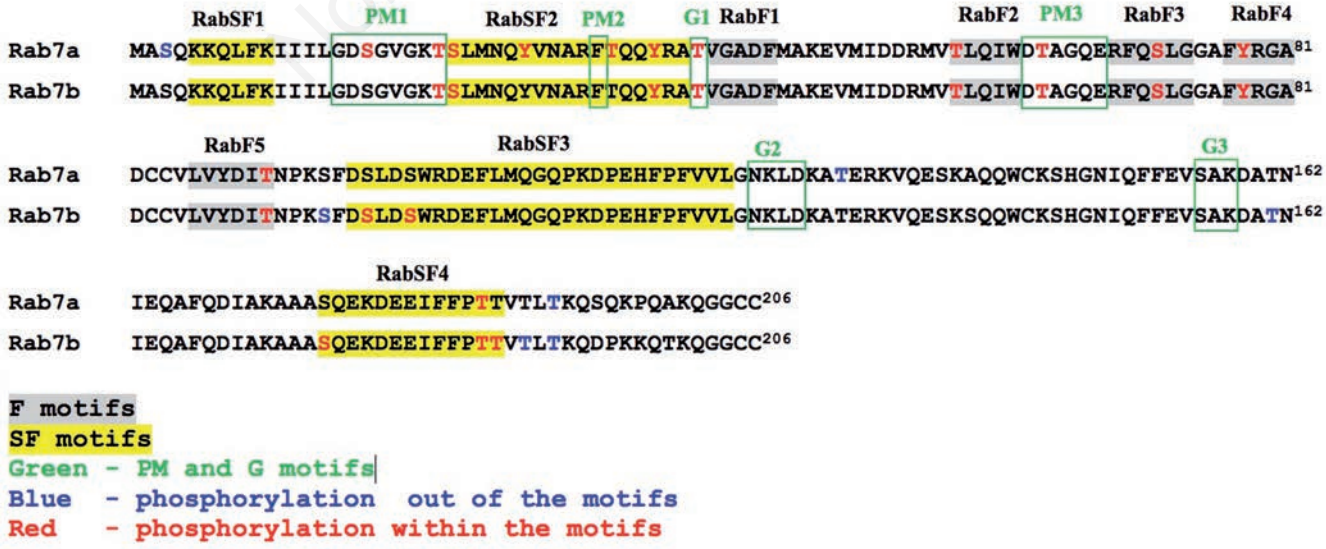

Figure 6. Phosphorylation patterns of *Paramecium octaurelia* Rab7a and Rab7b proteins detected by nano LC-MS/MS.

The following phosphorylations were detected beyond the Rab specific motifs: Thr192 in both the proteins and three in Rab7b (Ser95, Thr161, Thr190), whereas in Rab7a: Ser3 and Thr131. Interestingly, the following phosphorylation sites are in agreement with those predicted in Disphos 1.3 data base (http://www.dabi.temple.edu/disphos): in the case of Rab7b: Thr131, Ser176 and Thr188 (both in SF4), whereas in Rab7a only Thr131.

In vivo electroporation of *Paramecium* cells to deliver recombinant proteins

In order to examine intracellular targeting of recombinant $(His)_6$Rab7b proteins *Paramecium octaurelia* cells were electroporated in their presence under strictly controlled conditions as described in Materials and Methods. Double immunodetection under STED confocal microscopy with anti-His and anti-tubulin Abs revealed a proper localization of control recombinant $(His)_6$Rab7b to the cytostome area (Figure 7A) and mistargeting of $(His)_6$Rab7b_200 (Figure 7B), the deposits of which were seen in the cells. The two consecutive confocal optical slices shown in Figure 7 C-D clearly reveal the presence of recombinant control Rab7b at the edge of the cytostome, as shown earlier for endogenous Rab7b (compare Figure 6C in Osińska *et al*.[4]). Under a higher magnification tubulin association with the incorporated recombinant $(His)_6$Rab7b within the cytostome is visible in the cell (Figure 7E) in a pattern similar to that found for endogenous Rab7b in *Paramecium* (compare Figure 6 E in Osińska *et al*.[4]).

Discussion

Rab proteins involved in vesicular trafficking appeared early in evolution concomitantly with endomembranes, organelles and cell pathways evolution. They are involved in endocytosis, secretion, cell growth and differentiation,[3,9,20-26] and their paralogues have been reported.[6,7,27] Recent data indicate that diverse post-translational modifications could modify the functions of Rab proteins,[2,26,28,29] and we found that PTM of Thr200 located in the hypervariable C-terminal region of *Paramecium octaurelia* Rab7b determines its proper intracellular targeting and function.

The presence of *O*-linked carbohydrates in Rab7b protein explains the discrepancy between the predicted molecular weight of Rab7b and its observed M_r in SDS-PAGE also confirming our previous results from 2D gel electrophoresis that revealed two Rab7b immunoreactive spots at slightly different pI values, one of which was glycosylated,[4] similarly to bradykinin receptor B2.[30] It has also been shown that glycosylated proteins play a role in communication events.[31] Kudlow[32] pointed out that glycosylation, abundant and reversible, may evoke changes in protein functioning, whereas alternative *O*-glycosylation/*O*-phosphorylation of serine-16 in murine estrogen receptor beta has been shown to alter its stability.[33]

Recently, it has been shown that Rab7b (a new member of mammalian Rabs, displaying 54% identity to human Rab7a)[34] involved in retrograde transport from endosomes to the trans-Golgi network[35] and trafficking of several receptors,[36] coordinates cytoskeletal organization by influencing myosin light chain phosphorylation.[37] Our previous results clearly demonstrated that Rab7b was mapped to a cytoskeleton of the structure described as cytostome in *Paramecium* as seen in Figure 6D in Osińska *et al*.,[4] while the present study shows that point mutagenesis at Thr 200 preventing PTM abolishes this targeting.

According to Amoutzias and co-workers,[38]

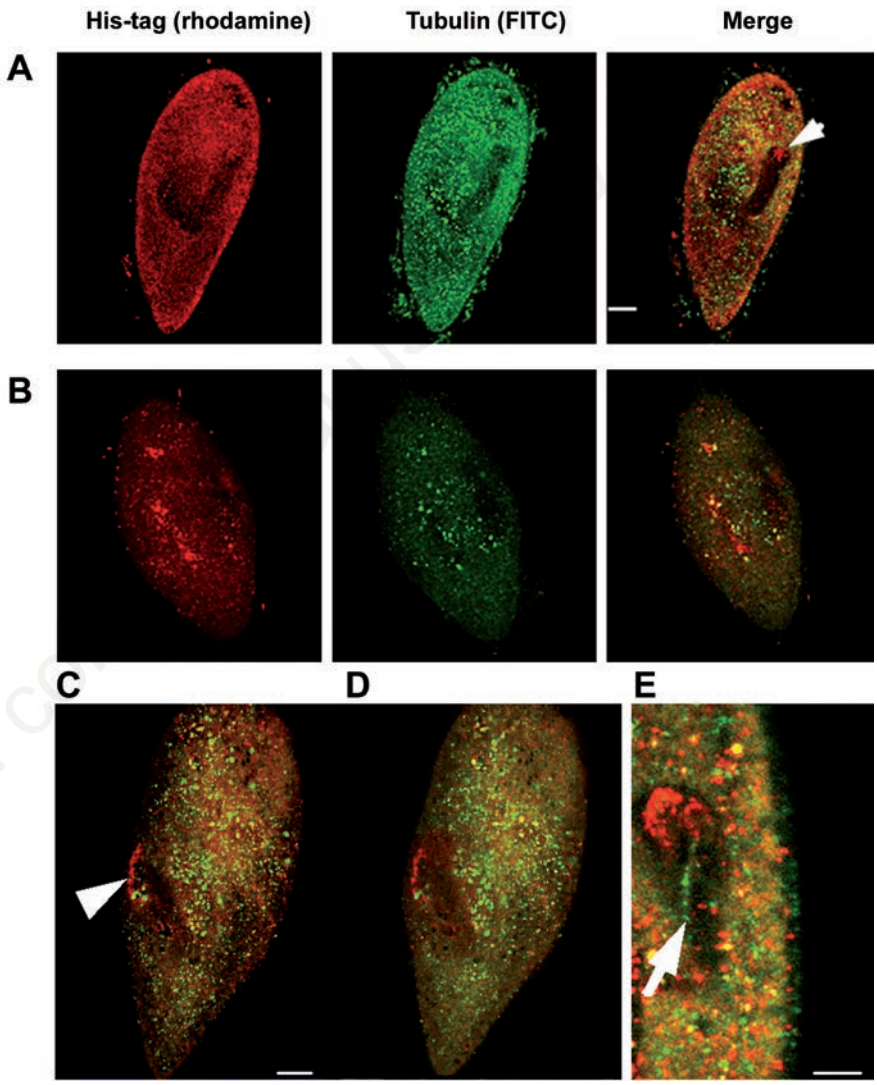

Figure 7. *In vivo* incorporation of recombinant proteins $(His)_6$Rab7b and $(His)_6$Rab7b_200 into electroporated *Paramecium octaurelia* cells. Immunolocalization in a STED confocal microscope. Recombinant proteins detected with anti-His antibody conjugated with rhodamine (red), detection of tubulin with antibody conjugated with FITC (green). A) $(His)_6$Rab7b, incorporation of the recombinant protein within the cytostome area (arrow). B) $(His)_6$Rab7b_200; please note dispersed incorporation of the protein; scale bars: 10 µm. C,D,E) $(His)_6$Rab7b. C,D) Two consecutive confocal optical slices (1 µm) showing accumulation of $(His)_6$Rab7b at the edge of the cytostome (white arrowhead); scale bars: 10 µm. E) Tubulin association with the incorporated control recombinant $(His)_6$Rab7b protein within the cytostome is visible at higher magnification (white arrow); scale bars: 5 µm.

phosphoproteins are more ancient, more abundant, have more protein interactions partners and are under tighter post-translational regulation than non–phosphorylated proteins. Phosphorylation of Rab proteins from diverse species has been reported including that of Rab1 and Rab4 in mitosis altering their association with membranes.[40-42] An interesting example of cyclic and reversible post-translational modification of Rab4 in CHO cells was reported by van der Sluijs and coworkers: this protein is phosphorylated during mitosis by Cdk1 when its large fraction accumulates in the cytosol whereas upon exit of cells from mitosis it undergoes dephosphorylation and reassociation with the membranes.[41] Phosphorylation of many Rab proteins has been reviewed by Bucci and Chiariello: using a great variety of methods they found that in three Rab5 isoforms a common phosphorylation site for Ser/Thr kinases is differentially recognized *in vitro* by specific kinases.[43] These isoforms are involved in early endocytic events of many markers and PTM could specifically modulate their function *in vivo.*[28] Furthermore, through interactions with Rab proteins, cargos directly control their own fate: a cargo protein has the ability to interact with more than one Rab and/or with the same Rab in different activation states.[44] In *Schizosaccharomyces pombe* two Rab7 homologs, Ypt7 and Ypt71, play antagonistic roles in the regulation of vacuolar morphology, whereas phosphorylation of the Rab protein Sec4 has been reported to prevent interactions with its effector and thus controlling exocyst function.[45,46] Phosphorylation of two amino acid residues in Rab7b that we detected within the RabSF3 motif, one of the regions required for GEF binding,[45,47] may influence such an interaction with an as yet unknown effector.

Thr200 phosphoglycosylation in *Paramecium* Rab7b was abolished by alanine substitution and could be removed by enzymatic deglycosylation with a mixture of five enzymes of different specificity as was done for nano- LC-MS/MS. Interestingly, tyrosine phosphorylation of Rab24 in cultured mammalian cells HEK293 and HEp-2 was reduced by alanine substitution of two consensus phosphorylation motifs: one in the hypervariable domain (as in the case of *Paramecium octaurelia* Rab7b) and the other within the motif known as the P-loop (Y17).[29] The latter region is known to influence GTP hydrolysis in Rab proteins, so the phosphorylation of Y17 could contribute to the low intrinsic GTPase activity of Rab24. Recent data[48] show that the hypervariable C-terminal domain (HVD) of Rab7 is required for proper targeting, unlike the HVD of Rab1 and Rab5 that is dispensable for membrane targeting and appears to function simply as a linker between the GTPase domain and the membrane. The N-terminal residues of Rab7 HVD are important for late endosomal/lysosomal localization.[48] We identified here an additional phosphorylation in *Paramecium* Rab7b in this region at Thr 191, within the Rab SF4 motif,[49] which did not occur in Rab7a (Figure 6). Interestingly, PTM plays also an important role in *Paramecium* exocytosis: an essential protein in this process is parafusin[50] associated with dense secretory vesicles that undergoes phosphoglucosylation prior to exocytosis and upon its deglycosylation, secretion occurs.[51] Exocytosis is totally blocked upon parafusin down-regulation by RNAi.[52] Recent studies indicate that parafusin is a signaling scaffold protein between nucleus and cilia and emerged early in eukaryotic evolution.[53] We reported previously that expression of Rab7a was 2.6-fold higher than that of Rab7b using qReal-Time PCR analysis.[4] Interestingly, this fact may be related to the recent data[54] on the evolution of two sodium channel paralogues following the teleost-specific WGD, indicating that the *Scn4ab* gene has a greater propensity toward neofunctionalization due to its decreased expression relative to its paralogue *Scn4aa*. Moreover, Amoutzias *et al*.[2] analyzing genome and phosphoproteome of *Saccharomyces cerevisiae* (which uderwent WGD), reported that post-translational regulation impacts the fate of duplicated genes and the number of phosphorylation sites on the proteins they encode is a major determinant of gene retention. In *Paramecium octaurelia* neofunctionalization of a product of the duplicated Rab7 genes is related to PTM of Thr200 in Rab7b which determines its targeting and putative interaction with bundles of microtubules and structures supporting the oral apparatus.[4] We show that upon mutagenesis of Rab7b this targeting is abolished.

References

1. Axelsen JB, Yan KK, Maslov S. Parameters of proteome evolution from histograms of amino-acid sequence identities of paralogous proteins. Biol Direct 2007;2:32.
2. Amoutzias GD, He Y, Gordon J, Mossialos D, Oliver SG, Van de Peer Y. Posttranslational regulation impacts the fate of duplicated genes. Proc Natl Acad Sci USA 2010;107:2967-71.
3. Mackiewicz P, Wyroba E. Phylogeny and evolution of Rab7 and Rab9 proteins. BMC Evol Biol 2009;9:101.
4. Osińska M, Wiejak J, Wypych E, Bilski H, Bartosiewicz R, Wyroba E. Distinct expression, localization and function of two Rab7 proteins encoded by paralogous genes in a free-living model eukaryote. Acta Biochim Pol 2011;58:597-607.
5. Aury J-M, Jaillon O, Duret L, Noel B, Jubin C, Porcel B, et al. Global trends of whole-genome duplications revealed by the ciliate Paramecium tetraurelia. Nature 2006;444:171-8.
6. Surmacz L, Wiejak J, Wyroba E. Cloning of two genes encoding Rab7 in Paramecium. Acta Biochim Pol 2006;53:149-56.
7. Ali BR, Seabra MC.Targeting of Rab GTPases to cellular membranes. Biochem Soc Trans 2005;33:652-6.
8. Pfeffer SR. Rab GTPase regulation of membrane identity. Curr Opin Cell Biol 2013;25:414-9.
9. Pereira-Leal JB, Seabra MC. The mammalian Rab family of small GTPases: definition of family and subfamily sequence motifs suggests a mechanism for functional specificity in the Ras superfamily. J Mol Biol 2000;301:1077-87.
10. Steentoft C, Vakhrushev SY, Joshi HJ, Kong Y, Vester-Christensen MB, Schjoldager KT, et al. Precision mapping of the human O-GalNAc glycoproteome through Simple Cell technology. EMBO J 2013;32:1478-88.
11. Soldo AT, Godoy GA, van Wagtendonk WJ. Growth of particle-bearing and particle-free Paramecium aurelia in axenic culture. J Protozool 1966;13:492-7.
12. Wyroba E, Bottiroli G, Giordano P. Autofluorescence of axenically cultivated Paramecium aurelia. Acta Protozool 1981; 20:165-70.
13. Wąsik R, Wińska P, Poznański J, Shugar D. Isomeric mono-, di-, and tri-bromobenzo-1H-triazoles as inhibitors of human protein kinase CK2α. PLoS One 2012;7: e48898.
14. Wiejak J, Surmacz L, Wyroba E. Dynamin- and clathrin-dependent endocytic pathway in unicellular eukaryote Paramecium. Biochem. Cell Biol 2004;82:547-58.
15. Suder P, Bodzon-Kulakowska A, Mak P, Bierczynska-Krzysik A, Daszykowski M, Walczak B, et al. The proteomic analysis of primary cortical astrocyte cell culture after morphine administration. J Proteome Res 2009;8:4633-40.
16. Noga M, Lewandowski JJ, Suder P, Silberring J. An enhanced method for peptide sequencing by N-terminal derivatization and MS. Proteomics 2005;5:4367-75.
17. Drabik A, Bodzon-Kulakowska A, Suder P. Application of the ETD/PTR reactionsin top-down proteomics as a faster alternative to bottom-up nanoLC-MS/MS protein identification. J Mass Spectrom 2012;47: 1347-52.
18. Cooper CA, Gasteiger E, Packer NH.

GlycoMod - a software tool for determining glycosylation compositions from mass spectrometric data. Proteomics 2001;1: 340-9.
19. Cooper CA, Gasteiger E, Packer N. (2003) Predicting glycan composition from experimental mass using GlycoMod. In: PM Conn (ed.) Handbook of proteomic methods. Humana Press, Totowa, USA: 2003.
20. Chavrier P, Gorvel JP, Stelzer E, Simons K, Gruenberg J, Zerial M. Hypervariable C-terminal domain of rab proteins acts as a targeting signal. Nature 1991;353:769-72.
21. Bucci C, Parton RG, Mather IH, Stunnenberg H, Simons K, Hoflack B, et al. The small GTPase rab5 functions as a regulatory factor in the early endocytic pathway. Cell 1992;70:715-28.
22. Zerial M, McBride H. Rab proteins as membrane organizers. Nat Rev Mol Cell Biol 2001;2:107-17.
23. Elias M, Brighouse A, Gabernet-Castello C, Field MC, Dacks JB. Sculpting the endomembrane system in deep time: high resolution phylogenetics of Rab GTPases. J Cell Sci 2012;125:2500-8.
24. Stenmark H. The Rabs: a family at the root of metazoan evolution. BMC Biol 2012; 10:68.
25. Diekmann Y, Seixas E, Gouw M, Tavares-Cadete F, Seabra MC, Pereira-Leal JB. Thousands of rab GTPases for the cell biologist. PLoS Comput Biol 2011;7:e1002217.
26. Park HH. Structural basis of membrane trafficking by rab family small g protein. Int J Mol Sci 2013;14:8912-23.
27. Dacks JB, Poon PP, Field MC. Phylogeny of endocytic components yields insight into the process of nonendosymbiotic organelle evolution. Proc Natl Acad Sci USA 2008; 105:588-93.
28. Chiariello M, Bruni CB, Bucci C. The small GTPases Rab5a, Rab5b and Rab5c are differentially phosphorylated in vitro. FEBS Lett 1999;453:20-4.
29. Ding J, Soule G, Overmeyer JH, Maltese WA. Tyrosine phosphorylation of the Rab24 GTPase in cultured mammalian cells. Biochem Biophys Res Commun 2003;312: 670-5.
30. Yaqoob M, Snell CR, Burgess GM. Carbohydrate analysis of the B2 bradykinin receptor from rat uterus. J Neurochem 1995;65:1290-6.
31. Davis BG, Lloyd RC, Jones JB. Controlled site-selective protein glycosylation for precise glycan structure-catalytic activity relationships. Bioorg Med Chem 2000;8:1527-35.
32. Kudlow JE. Post-translational modification by O-GlcNAc: another way to change protein function. J Cell Biochem 2006;98:1062-75.
33. Cheng X, Hart GW. Alternative O-glycosylation/O-phosphorylation of serine-16 in murine estrogen receptor beta: post-translational regulation of turnover and transactivation activity. J Biol Chem 2001;276: 10570-5.
34. Yang M, Chen T, Han C, Li N, Wan T, Cao X. Rab7b, a novel lysosome-associated small GTPase, is involved in monocytic differentiation of human acute promyelocytic leukemia cells. Biochem Biophys Res Commun 2004;318:792-9.
35. Progida C, Cogli L, Piro F, De Luca A, Bakke O, Bucci C. Rab7b controls trafficking from endosomes to the TGN. J Cell Sci 2010;123:1480-91.
36. Bucci C, Bakke O, Progida C. Rab7b and receptors trafficking. Commun Integr Biol 2010;3:401-4.
37. Borg M, Bakke O, Progida C. A novel interaction between Rab7b and actomyosin reveals a dual role in intracellular transport and cell migration. J Cell Sci 2014; 127:4927-39.
38. Amoutzias GD, He Y, Lilley KS, Van de Peer Y, Oliver SG. Evaluation and properties of the budding yeast phosphoproteome. Mol Cell Proteomics 2012;11:1-13.
39. Barr FA. Review series: Rab GTPases and membrane identity: causal or inconsequential? J Cell Biol 2013;202:191-9.
40. Bailly E, McCaffrey M, Touchot N, Zahraoui A, Goud B, Bornens M. Phosphorylation of two small GTP-binding proteins of the Rab family by p34cdc2. Nature 1991;350:715-8.
41. van der Sluijs P, Hull M, Huber LA, Mâle P, Goud B, Mellman I. Reversible phosphorylation-dephosphorylation determines the localization of rab4 during the cell cycle. EMBO J 1992;11:4379-89.
42. Uno T, Nakao A, Katsurauma C. Phosphorylation of Rab proteins from the brain of Bombyx mori. Arch Insect Biochem Physiol 2004;57:68-77.
43. Bucci C, Chiariello M. Signal transduction gRABs attention. Cell Signal 20016;18:1-8.
44. Aloisi AL, Bucci C. Rab GTPases-cargo direct interactions: fine modulators of intracellular trafficking. Histol Histopathol 2013;28:839-49.
45. Kashiwazaki J, Iwaki T, Takegawa K, Shimoda C, Nakamura T. Two fission yeast rab7 homologs, ypt7 and ypt71, play antagonistic roles in the regulation of vacuolar morphology. Traffic 2009;10:912-24.
46. Heger CD, Wrann CD, Collins RN. Phosphorylation provides a negative mode of regulation for the yeast Rab GTPase Sec4p. PLoS One 2011;6:e24332.
47. Day GJ, Mosteller RD, Broek D. Distinct subclasses of small GTPases interact with guanine nucleotide exchange factors in a similar manner. Mol Cell Biol 1998;18: 7444-54.
48. Li F, Yi L, Zhao L, Itzen A, Goody RS, Wu YW. The role of the hypervariable C-terminal domain in Rab GTPases membrane targeting. Proc Natl Acad Sci USA 2014;111: 2572-7.
49. Diekmann Y, Pereira-Leal JB. Bioinformatic approaches to identifying and classifying Rab proteins. Methods Mol Biol. 2015:1298:17-28.
50. Subramanian SV, Wyroba E, Andersen AP, Satir BH. Cloning and sequencing of parafusin, a calcium-dependent exocytosis-related phosphoglycoprotein. Proc Natl Acad Sci USA 1994;91:9832-6.
51. Subramanian SV, Satir BH. Carbohydrate cycling in signal transduction: parafusin, a phosphoglycoprotein and possible Ca(2+)-dependent transducer molecule in exocytosis in Paramecium. Proc Natl Acad Sci USA 1992;89:11297-301.
52. Liu L, Wyroba E, Satir BH. RNAi knockdown of parafusin inhibits the secretory pathway. Eur J Cell Biol 2011;90:844-53.
53. Satir BH, Wyroba E, Liu L, Lethan M, Satir P, Christensen ST. Evolutionary implications of localization of the signaling scaffold protein Parafusin to both cilia and the nucleus. Cell Biol Int 2015;39:136-45.
54. Thompson A, Vo D, Comfort C, Zakon HH. Expression evolution facilitated the convergent neofunctionalization of a sodium channel gene. Mol Biol Evol 2014; 31:1941-55.